Geologos 22, 3 (2016): 201–211
doi: 10.1515/logos-2016-0021

GEOLOGOS

# Soft-sediment deformation structures in cores from lacustrine slurry deposits of the Late Triassic Yanchang Fm. (central China)

Renchao Yang[1], A.J. (Tom) van Loon[2*], Wei Yin[3], Aiping Fan[1] & Zuozhen Han[1]

[1]Shandong Provincial Key Laboratory of Depositional Mineralization & Sedimentary Minerals, Shandong University of Science and Technology, Qingdao 266590, China;
e-mail addresses: yang100808@126.com (RY), xiaofan781026@sina.com (AF), hanzz@163.com (ZH)
[2]Geocom Consultants, Valle del Portet 17, 03726 Benitachell, Spain; e-mail: Geocom.VanLoon@gmail.com
[3]Sinopec Petroleum Exploration & Production Research Institute, Beijing 100083, China;
e-mail: yinwei.syky@sinopec.com
[*]Corresponding author

**Abstract**

The fine-grained autochthonous sedimentation in the deep part of a Late Triassic lake was frequently interrupted by gravity-induced mass flows. Some of these mass flows were so rich in water that they must have represented slurries. This can be deduced from the soft-sediment deformation structures that abound in cores from these lacustrine deposits which constitute the Yanchang Fm., which is present in the Ordos Basin (central China).
The flows and the resulting SSDS were probably triggered by earthquakes, volcanic eruptions, shear stress of gravity flows, and/or the sudden release of overburden-induced excess pore-fluid pressure. The tectonically active setting, the depositional slope and the high sedimentation rate facilitated the development of soft-sediment deformations, which consist mainly of load casts and associated structures such as pseudonodules and flame structures. Sediments with such deformations were occasionally eroded by slurries and became embedded in their deposits.

**Keywords:** soft-sediment deformation structures, low-density gravity-flow deposits, Triassic, lacustrine sediments, Ordos Basin, China

## 1. Introduction

The Ordos Basin in central China is rich in unconventional hydrocarbons. These occur mainly in fine-grained lithified sediments, such as shales, mudstones and siltstones (Schieber, 1994; Schieber et al., 2007; Hovikoski et al., 2008; Bhattacharya & MacEachern, 2009; Aplin & Macquaker, 2011; Plint, 2014; Kostic, 2014). Part of the hydrocarbons occur in the lacustrine shales of the Triassic Yanchang Formation, which has been dated as Late Triassic.

The occurrence of the hydrocarbons has raised considerable interest in this formation, and many wells have been drilled. Numerous cores were investigated in detail, and it has turned out that the lacustrine Yanchang Fm. represents the deeper part of a lake where sedimentation took place largely by settling of fine particles from suspension, with minor contributions by bottom currents that left small-scale, sometime fine-sandy, current ripples. This quiet picture was interrupted fairly frequently, however, by mass flows of different types, ranging from hyperpycnal flows and turbidity currents to high-density debris flows. This wide spectrum of mass flows included numerous other types, such as plug flows, quasi-laminar plug flows and tran-

sitional plug flows, which probably passed occasionally into each other, progressively changing their character along the transport path, with transformation primarily resulting from reductions in sediment concentration through progressive entrainment of surrounding fluid and/or sediment deposition (cf. Mulder & Alexander, 2001). All flow types left their specific traces in the form of lateral extent, thickness, grain-size distribution and sedimentary structures.

In the present contribution we focus on flows with such a high water content and such fine-grained particles, that they should be considered as slurries. Whereas the general term 'fluid mud' is defined as a bottom-hugging mobile subaqueous body of fine-grained sediments with a concentration of solids > 10 $g \cdot L^{-1}$ (Kirby & Parker, 1983), which consists primarily of clay- and silt-sized-particles with variable amounts of organic material (Ichaso & Dalrymple, 2009), the term `slurry flow' is used to refer to watery flows transitional between turbidity currents and debris flows; most slurry-flow deposits have a matrix of 10±35% of detrital mud matrix and are grain-supported (Lowe & Guy, 2000). A slurry flow is defined in the present contribution as a sediment that has undergone mass transport with an ultra-high concentration of insoluble particles (such as sand, silt, marl and/or clay) of over 500 $g \cdot L^{-1}$ and that was driven by gravity.

Like the other types of mass flows, slurries move downslope until their momentum is no longer sufficient – due to a gradual decrease of the sedimentary slope – to continue flowage. The resulting slurry deposits are extremely water-rich and prone to deformation, particularly due to the fine grain size of the constituting particles, which is caused by the gradual loss of coarser material during transport as a slurry (cf. Lowe et al., 2003). This results in the frequent occurrence of soft-sediment deformation structures (SSDS; this acronym is used here for both singular and plural), which differ in their characteristics from SSDS formed in soft sediments with a lower water content and a granulometry that is less susceptible to deformation.

Although much research on gravity flows has been carried out during the past few decades, the relationship between gravity flows and their depositional characteristics is still insufficiently understood (Sumner et al., 2009; Lamb & Mohrig, 2009; Talling et al., 2007; Pouderoux et al., 2012), especially concerning fine-grained deposits. A study by Plint (2014) has clearly pointed out the difficulties of recognizing microstructures and understanding the transport processes that resulted in mudstones. We presume that more detailed studies of the SSDS in mass-transported fine-grained sediments can deepen the insight in the depositional conditions of such sediments, though it should be kept in mind that, in addition to the granulometry of the mass-transported sediments, also the water/particle ratio during transport and the pore-water content after deposition play a major role. We restrict our attention in the present contribution therefore to mass-transport processes in which so much water was involved that their deposits were initially saturated, if not over-saturated, with water. This may be of particular interest since Mesozoic deposits of water-rich flows on deltaic slopes and in deep lacustrine environments have rarely been documented.

## 2. Geological setting

The soft-sediment deformation structures in the slurry deposits under study here occur in the Late Triassic Yanchang Formation, which forms part of the succession filling the Ordos Basin. This basin is the second largest sedimentary basin in China (Fig. 1A), covering 320,000 $km^2$. Being situated on a stable Archaean crystalline basement, it developed during the Mesoproterozoic, but sediments accumulated up till the Tertiary. These are on average 4–5 km thick, but the thickness varies from place to place (Zou et al., 2012; Yang & Deng, 2013).

Palaeocontinents in the south were one of the main source areas of the Yanchang Fm. during the Late Triassic, thanks to uplift caused by the collision of the South China and the Sino-Korea Blocks (Weislogel et al., 2006; Dong et al., 2012. The collision and thrusting downwarped the Ordos Basin, resulting in slopes on both sides of 3.5–5.5° in the south and 1.5–2.5° in the north (Fig. 1B). Fast subsidence of the basement and deepening of the basin resulted in a transgression of the lake during the early Late Triassic. The combination of rapid uplift, steep slopes, a humid climate, and a location close to the source area was favourable for the triggering of gravity flows.

The Yanchang Fm. consists of detrital fluvial/deltaic/lacustrine sediments of 1000–1300 m thick. Fossils in the Yanchang Fm. indicate that the Ordos Basin was located at low latitude with a warm and humid climate (Ji et al., 2010). During the late Middle Triassic, a shallow lake and deltas developed, as indicated by alternations of fine sandstones and mudstones. The lake became deep in the early Late Triassic, as a result of fast subsidence of the basement. A succession of dark (kerogen-rich) deep lacustrine shales with thicknesses of 20–80 m subsequently developed in the more central part of the

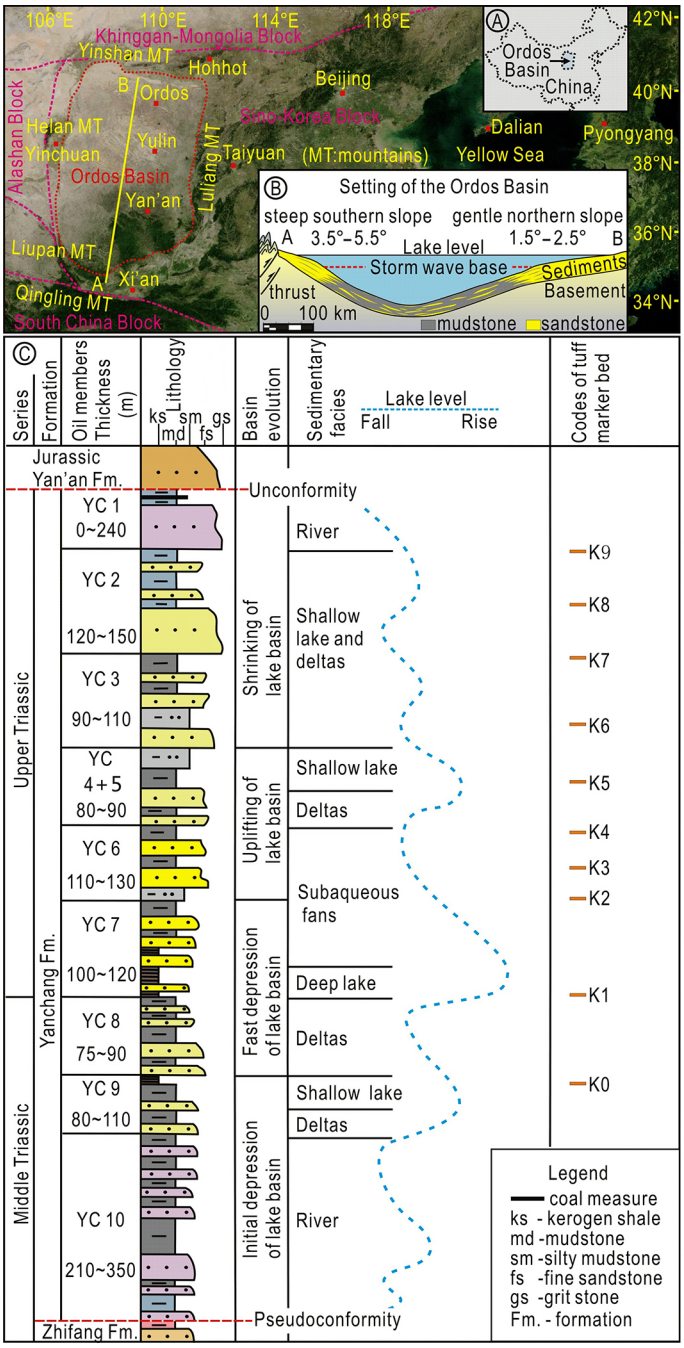


**Fig. 1.** Location (A), geological setting (B) and Triassic succession (C) of the Ordos Basin. The main map shows the regional topography and the structural framework of central China, and the peripheral mountains of the Ordos Basin. The yellow line from A to B shows the location of the section sketched in (B). Inset map (B) shows the uplift of the Qinling Mountains, thrusts, downwarping and inclination of the Late Triassic basin. Figure (C) shows the Middle-Late Triassic strata, lithology and thicknesses of the 10 members (YC 1 to YC 10), lithofacies, lake-level fluctuations and basin evolution of the Yanchang Fm. Modified after Yang et al. (2016).

basin, whereas deltas developed in the southern and northern parts (Fig. 2). Intercalations of numerous tuffaceous beds between the dark shales point at frequent volcanic eruptions in the surrounding mountains; thin turbidity currents reached the deep lake and form also frequent intercalations between the autochthonous mudstones (Zou et al., 2012; Yang et al., 2014). Subsequently, the Ordos Lake became increasingly shallower during the Late Triassic. Lacustrine deltas and turbidite fans spread from the north and south to the central Ordos Basin. This resulted in the deposition of fine sandstones and mudstones (Deng et al., 2011; Zou et al., 2012; Yang & Deng, 2013).

## 3. Soft-sediment deformation structures in the lacustrine cores

The mudstones of the deep lacustrine Yanchang Fm. commonly (but not always) show lamination, but occasionally they are massive. Moreover, in numerous cores well-developed SSDS are present. Al-

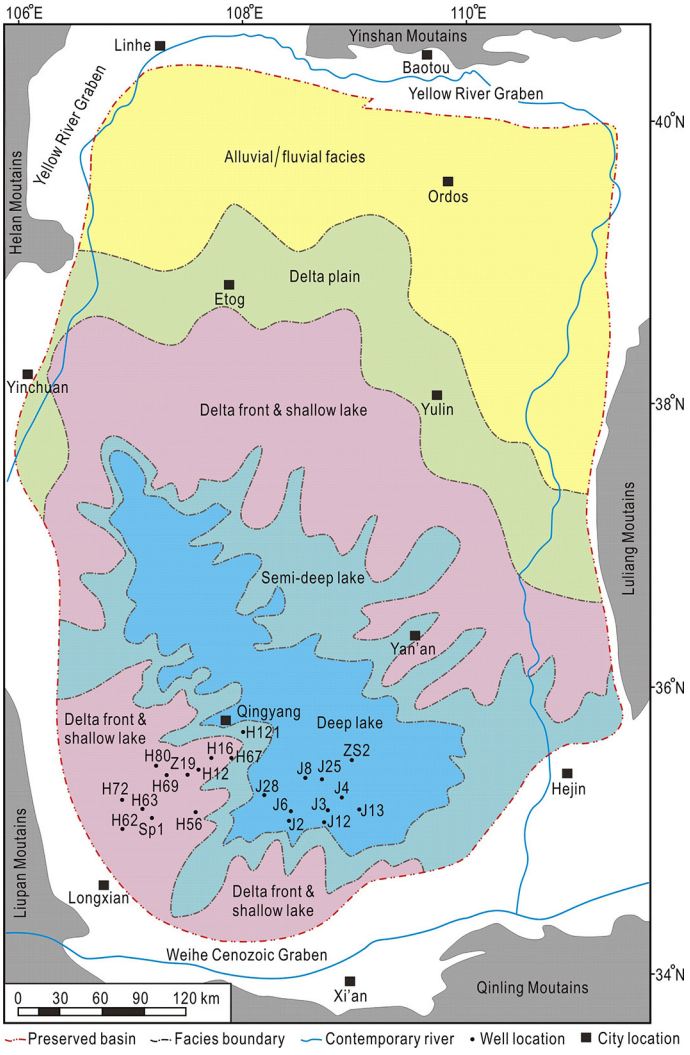


**Fig. 2.** Preserved extent of the Ordos Basin, and lithofacies of the member (YC 7) of the Yanchang Fm. under study here. The map also shows the mountains around the basin, and the well locations (codes H and J indicate the Honghe and Jinghe areas, respectively; the numbers indicate the well number for each area). Modified after Yang et al. (2016).

though cores offer the possibility to study the SSDS in 3-D, the interpretation of such deformations in cores remains difficult, although such SSDS from cores obtained from fine-grained lacustrine and paludal sediments have been described and analysed before (e.g. Ezquerro et al., 2015, 2016; Törö & Pratt, 2016). Most authors presume that seismic activity triggered the deformation processes.

Several types of SSDS are present in the mudstones of the Yanchang Fm. They represent the flow conditions (syndepositional SSDS) as well as the conditions at the sedimentary surface after deposition (metadepositional SSDS), and sometimes also after deposition of a next layer (postdepositional SSDS). Considering the relatively small lateral extent of the SSDS as far as visible in a core, interpretation of the deformational stage is not always reliably possible.

Numerous SSDS indicate a certain degree of consolidation of the mass-transported material during and/or after transport. This degree is best expressed by the nature of the deformations: they can point at brittle behaviour (faulting), at liquefaction (plastic deformation) and at fluidization (sand veins). It should be kept in mind, however, that also water-saturated, unconsolidated sediments can show faults, not only as a 'side-product' of plastic deformation, but also as a primary deformation that took place sufficiently rapidly (cf. Van Loon & Wiggers, 1975, 1976). Commonly SSDS of different types are found closely together, suggesting that the material had different properties during transport and/or deposition, which is a normal feature during mass-transport. An example is Figure 3, showing cm-scale faults, bent laminae and thin veins of fluidized sand.

Most SSDS in the mudstones are load casts or directly related structures, either or not deformed later. Load casts are the most common SSDS in lacustrine sediments and have been described and interpreted in numerous publications (Kuenen, 1958; Kelly & Martini, 1986; Rodríguez-López et al., 2007;

**Fig. 3.** Example of a core with a variety of small-scale soft-sediment deformation structures, including faults, bent laminae and intrusions of fluidised sediment. Core from well SP1, depth 1971.3 m.

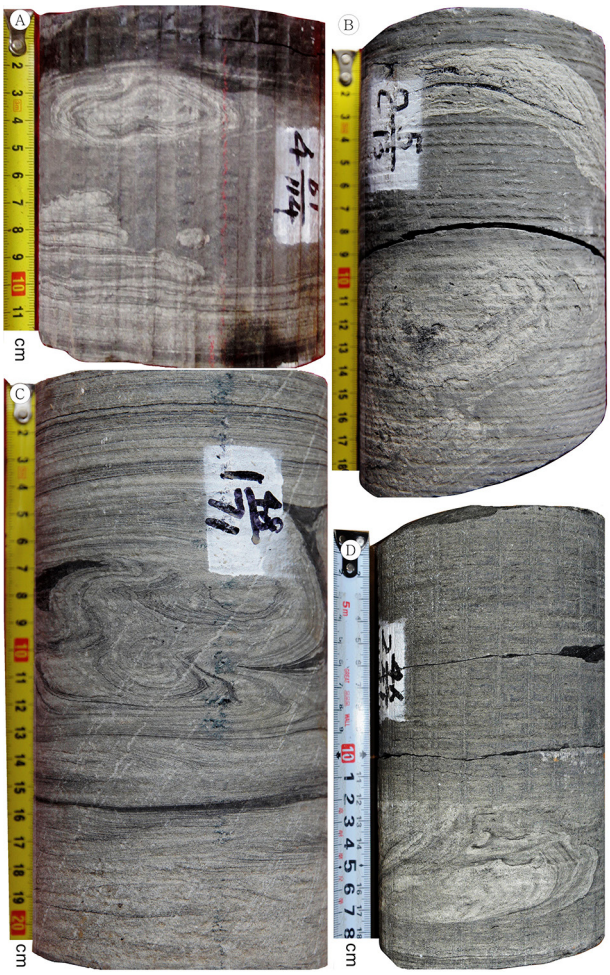

**Fig. 4.** Pseudonodules in various shapes. **A:** Characteristic pseudonodule derived from a fine-sandy layer that completely disappeared due to the loading process. Note the deformation in the lower part of the core. Core from well J25, depth 1348.7 m. **B:** Cross-section through a pseudonodule derived from a layer with similar lithology as the off white layer above it. It cannot be excluded that the pseudonodule was derived from this layer. Core from well H67, depth 1496.3 m. **C:** SSDS consisting of a combination of load casts and pseudonodules, probably caused by successive deformation phases. Core from well H121, depth 1755.1 m. **D:** Pseudonodule with repeated phases of deformation. Core from well H69, depth 1830.3 m.

Gladkov et al., in press). Many of the load casts in the Yanchang Fm. consist of fine-sandy material that has sunk into mud. Wherever the mud had already been somewhat consolidated, the load casts show 'classical' forms; where the mud was still fairly soft, the sandy material could easily sink farther downwards to become either pseudonodules (Fig. 4A,B) or deformed loads casts (Fig. 4C), often also deformed pseudonodules (Fig. 4D). Gravity flows with erosional capability were common, as expressed by the occurrence of lithic clasts (Fig. 5A). Such erosive flows also caused that some load casts became truncated at their top (Fig. 5B). Other processes that resulted in 'destruction' of loads casts are burrows of organisms that worked their way through the topmost sediments of the deep lake (Fig. 6).

From the point of view of soft-sediment deformation, the most interesting are the often chaotic deformations caused by the turbulent flow character of slurry flows, and by the weight of freshly deposited event layers on top of the water-saturated slurry deposits. These slurry flows consisted of failed sediment (cf. Sylvester & Lowe, 2004), most probably deposited originally on the sloping front of deltas that prograded in the lake. These relatively distal delta fronts were built of alternations of muds and fine sands, which started moving *en masse* downslope. There may have been several reasons for such failure, such as oversteepening due to the high accumulation rate, storm wave activity, tectonics (resulting in seismic shock waves) and shocks due to volcanic activity (Deng et al., 2011; Dong et al., 2012).

When the water-saturated slope sediments started to move downslope, increasingly more wa-

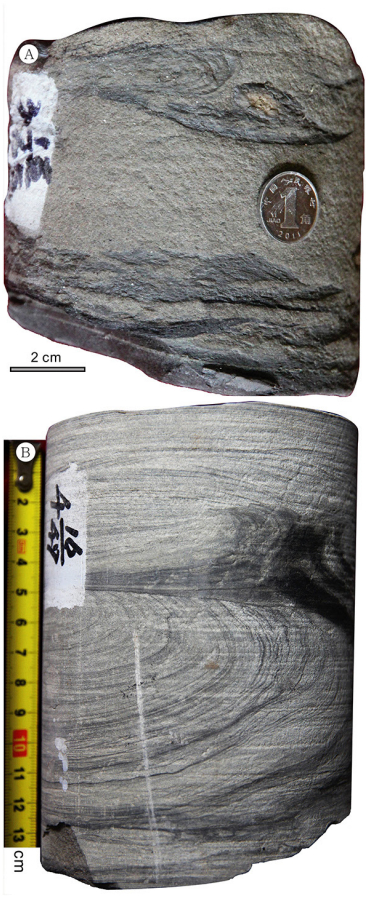


**Fig. 5.** Expressions of the erosional capability of some slurries. **A:** Lithic clasts at the base of a slurry deposit. Note the SSDS in the overlying layer. Core from well J12, depth 1246.8 m). **B:** Truncated load cast, caused by the erosive action of a subsequent slurry. Core from well H62, depth 2147.32 m.


**Fig. 6.** Burrow in an exposure of the same stratigraphic level of the Yanchang Fm. as under study in the present contribution. Xunyi County, Shaanxi Province.

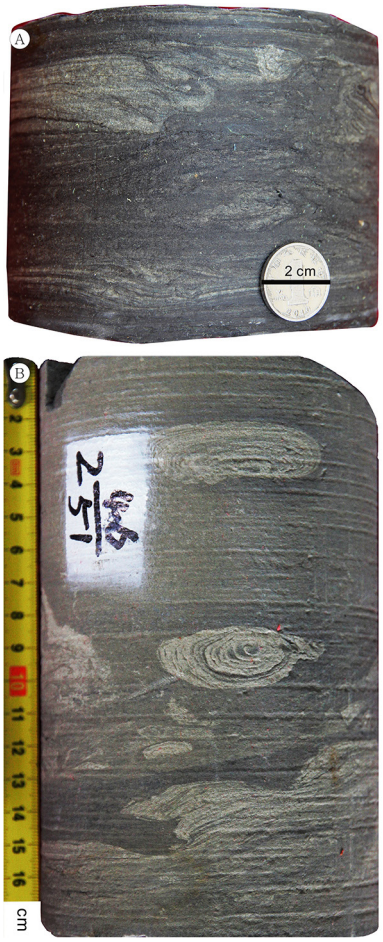


**Fig. 7.** Slurry deposits with floating soft-sediment masses of divergent lithology. **A:** Irregular distribution of fine-sandy, deformed sediment within a slurry deposit. Core from well J8, depth 1271.5 m. **B:** Floating pseudonodules and other sedimentary masses in a slurry deposit. Note that the upper pseudonodule is positioned upside down. Core from well H56, depth 1857.7 m).

ter was included, so that eventually a slurry was formed. The turbulent flow of the slurry led to erosion of the sedimentary bottom and of subaqueous natural levees that existed alongside the channels in the delta slope; part of these sediments may have been so water-saturated that the individual particles lost the contact with each other, so that they became mixed up with the other sediment particles in the slurry, thus increasing the erosional power of this flow. The increased erosional capability occasionally led to the erosion of more consolidated sediment. These became included in the slurry with its chaotic turbulent character, forming lumps that partly became deformed during transport, either by rolling over the sedimentary bottom, or by the powerful whirls in the slurry. This explains the occurrence in several cores of slurry deposits consisting

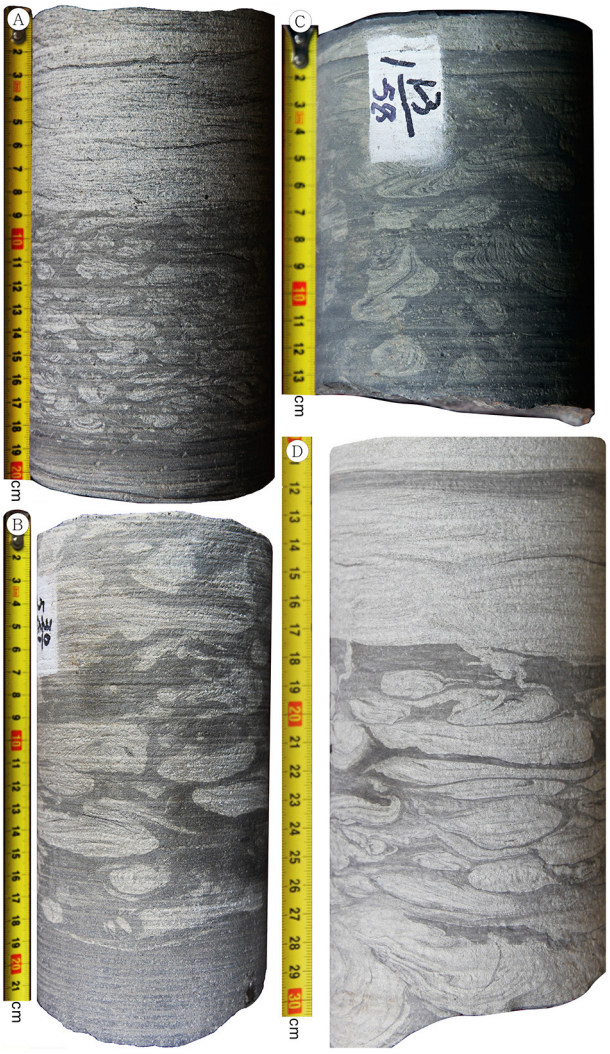

**Fig. 8.** Muddy slurry deposits consisting for a large part of lumps of deformed fine-sandy material, possibly derived from eroded bottom sediments, possibly consisting of fine-sandy layers in the muddy succession that started to flow downslope. **A:** Densely packed load casts, pseudonodules and other deformed sedimentary masses in a well-defined slurry deposit. Core from well H72, depth 2065.6 m. **B:** Rounded fragments of only slightly deformed sandy material in a muddy slurry deposit. Core from well H62, depth 2157.6 m. **C:** Another core with strongly contorted fine-sandy sediment lumps in a slurry deposit. Core from well H63, depth 2343.1 m. **D:** Densely packed, deformed fine-sandy sediment masses in a slurry deposit. Core from well H72, depth 2070.3 m.

predominantly of mud, in which deformed lumps of somewhat more sandy material are embedded, sometimes as floating, more or less isolated masses (Fig. 7), sometimes in quantities that are almost equal in volume as the mud matrix (Fig. 8).

The farther downslope slurry flows travelled, the less recognizable the individual lumps of eroded more sandy material became: the individual fragments were torn apart, bumped against each other, absorbed water, etc., so that they lost their original shapes and eventually became more or less shapeless masses (Fig. 9).

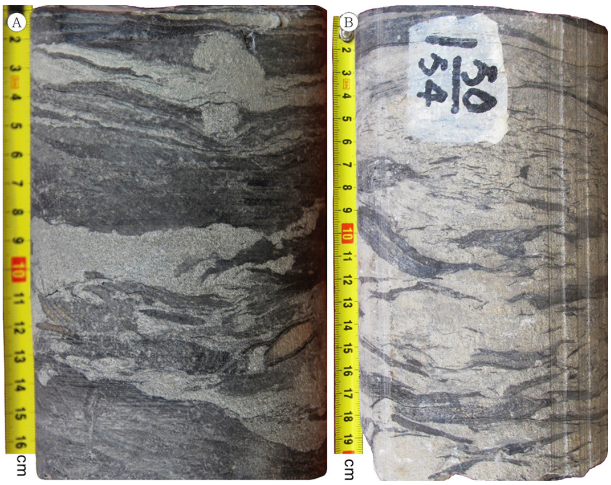

**Fig. 9.** Muddy slurry deposits with fairly shapeless masses of deformed fine-sandy material. **A:** Relatively thick slurry deposit with concentrations of fine-sandy material at several levels. Core from well J2, depth 1319.3 m. **B:** Densely packed, more or less bedding-parallel masses of fine-sandy deformed sediment in a relatively thick slurry deposit with a muddy matrix. Core from well ZS2, depth 1348.1 m.

## 4. Discussion

The various hydrodynamics and/or transporting-depositional mechanisms and processes controlled the nature of the sedimentary structures, textures and SSDS in the deep lacustrine muds that build the Yanchang Fm. On the other hand, these features can help to reconstruct the processes that prevailed in the sedimentary environment. The interpretation of the texturally heterogeneous mudstones in the Yanchang Fm. are based on these analyses, and it is deduced that most of the mudstones must be interpreted as slurry deposits in environments ranging from the sedimentary slope of a delta front to a lacustrine bottom. Other types of mass flows existed, however, as well, mainly in the form of muddy debris flows, fluidized mud flows, hybrid flows (cf. Haughton et al., 2009) and turbidites/hyperpycnites.

The sedimentary environments were relatively stable over a fairly long time, as can be inferred from the thickness of the lacustrine deposits. The delta-front and lacustrine environments were, however, fairly frequently affected by mass flows that

resulted in a large number of event deposits, mainly slurry deposits.

Various flow regimes must have existed, depending on the slope, the water/sediment ratio and the water turbulence of the flows. Varying amounts of disseminated sand, mudstone intraclasts and organic detritus indicate erosional capability of at least part of the flows. The rare bioturbation indicates relatively continuous sedimentation at a high rate rather than slow settling from dilute suspensions (cf. MacEachern et al., 2005; Neill & Allison, 2005; Bhattacharya & MacEachern, 2009). Most mudstone layers in the Yanchang Fm. are therefore interpreted as having been deposited rapidly in a relatively high-energy environment, rather than in low-turbulence still water, mostly in the form of gravity flows, such as turbidity currents, hyperpycnal flows, muddy debris flows and slurry flows. Plug flows, quasi-laminar plug flows and transitional plug flows must also have contributed.

The development of slurry deposits requires slope failure, which in turn requires both accumulation of much sediment and a trigger (Yao et al., 2012). The requirement of accumulation of much sediment was certainly fulfilled in the case of the sediments under study here, since so much clastic material was supplied that the delta front in the basin grew at a high rate. The requirement of a trigger was probably met as well. Mass flows commonly originate due to slope failure. This may be triggered by a wide variety of processes such as earthquakes, volcanic eruptions, storms and river floods (Sumner et al., 2012, 2013; Clare et al., 2014). Numerous tuff layers that are present within the deep lacustrine mudstones indicate that volcanoes erupted frequently near the Ordos Basin during the Late

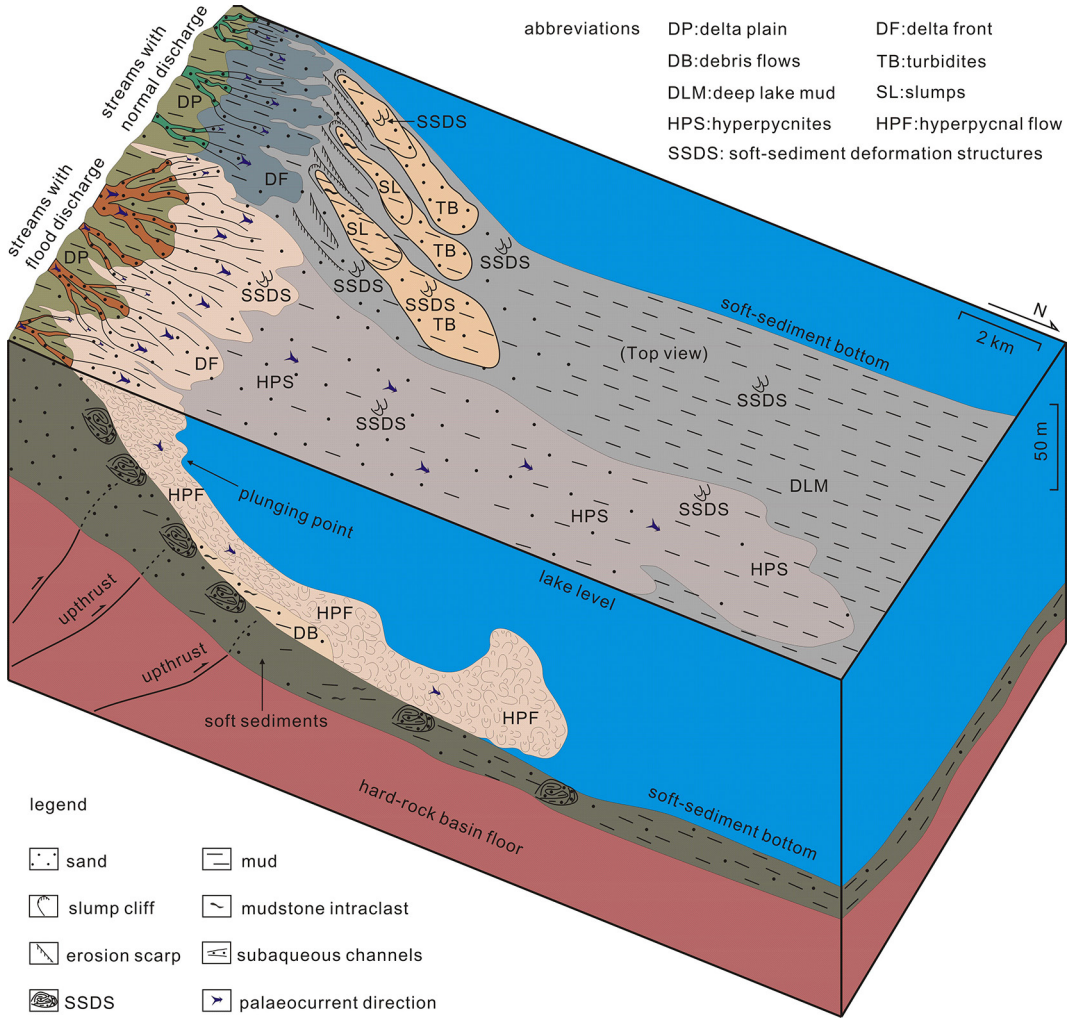


**Fig. 10.** Schematic block diagram showing the depositional environment, the depositional processes and the distribution of the resulting sediments, and the distribution of the soft-sediment deformation structures of the types found in the cores under study.

Triassic (Yang et al., 2014). Clay-rich sediment gravity flows played an important role in the sedimentary environment from the delta front to the deep lacustrine area in the Ordos Basin. Clays contribute to the weakness of beds as they are highly sensitive to deformation (Hansen et al., 2011). The clay-rich unconsolidated sediments on the delta slope were consequently prone to deform, slide and slump, so as to initiate slurry flows.

SSDS can be generated by a wide variety of geological agents, such as liquefaction or fluidization by earthquake-induced shock waves (e.g., Martín-Chivelet et al., 2011; Berra & Felletti, 2011), adjustment to gravity in successions with reversed density gradients (e.g., Mills, 1983), shear stress (e.g., Mills, 1983), sudden overloading by mass-transported sediments (e.g., Callot et al., 2008), slumping or slope failure (e.g., Yang et al., 2014; Alves, 2015). In most cases a combination of these mechanisms must be held responsible for the SSDS (Mills, 1983). Large-scale deformations often appear to result from tectonic activity (Van Loon, 2002; Ghosh et al., 2002), whereas deformations of intermediate or smaller size commonly result from exogenic processes such as glaciotectonism, overburden-induced diapirism and numerous other processes (Van Loon, 2002).

Liquefaction and fluidization by earthquake-induced shock waves probably played an important – if not critical – role in the generation of SSDS in the Yanchang Fm. during the Late Triassic, when the Ordos Basin was tectonically active, as shown by characteristic deformations. Volcanic eruptions and the consequent sudden overloading by volcanoclastics may also have generated deformation of the still soft sediments on the delta slope, judging from the presence of tuffaceous mudstones (associated with SSDS). Other SSDS originated during downslope movement.

Pore-fluid migration and an increase in pore-fluid pressure can be critical for slope instability and can trigger slope failure, especially within sediments close to the critical state (Yamamoto, 2014). A high depositional rate, low permeability and low shear strength within fine-grained deposits provide the best conditions for the occurrence of SSDS in the Yanchang Fm. (cf. Callot et al., 2008; Yang et al., 2014). These water-saturated, clay-rich sediments were prone to liquefaction and fluidization, allowing them to act as a lubricant that facilitated downslope movement over the delta slopes in the Ordos Basin, so inducing numerous deformations. This implies that a sudden release of the overburden-induced pore pressure in the sediments on the delta slopes where the sedimentation rate was high, must be held responsible for of the majority of the SSDS in the sediments under study (Fig. 10).

## 5. Conclusions

Subaqueous gravity flows transported and deposited mainly fine-grained particles such as silt and mud on the slopes of delta fronts and in the deep lacustrine areas of the Ordos Basin during the Late Triassic. These event deposits occur frequently intercalated between the autochthonous mudstones. Many of the flows had the characteristics of slurries, and their deposits contain abundant soft-sediment deformation structures that reflect these flows and depositional conditions.

The flows and the resulting SSDS may have been triggered by earthquakes, volcanic eruptions, shear stress of gravity flows, and/or the sudden release of overburden-induced excess pore-fluid pressure. A tectonically active setting, a depositional slope and a high sedimentation rate facilitated the development of soft-sediment deformations on the lacustrine delta fronts. Alternations of water-saturated sands and soft muds with, consequently, reversed density gradients were additional favourable factors for deformation processes.

**Acknowledgements**

This study was supported by the National Natural Science Foundation of China (Grants No. 41372135 and No. 41672120) and by the SDUST Research Fund (Grant No. 2015TDJH101).

## References

Alves, T.M., 2015. Submarine slide blocks and associated soft-sediment deformation in deep-water basins: A review. *Marine and Petroleum Geology* 67, 262–285.

Aplin, A.C. & Macquaker, J.H.S., 2011. Mudstone diversity: origin and implications for source, seal, and reservoir properties in petroleum systems. *American Association of Petroleum Geologists Bulletin* 95, 2031–2059.

Berra, F. & Felletti, F., 2011. Syndepositional tectonics recorded by soft-sediment deformation and liquefaction structures (continental Lower Permian sediments, Southern Alps, Northern Italy): Stratigraphic significance. *Sedimentary Geology* 235, 249–263.

Bhattacharya, J.P. & MacEachern, J.A., 2009. Hyperpycnal rivers and prodeltaic shelves in the Cretaceous Seaway of North America. *Journal of Sedimentary Research* 79, 184–209.

Callot, P., Odonne, F. & Sempere, T., 2008. Liquification and soft-sediment deformation in a limestone mega-

breccia: The Ayabacas giant collapse, Cretaceous, southern Peru. *Sedimentary Geology* 212, 49–69.

Clare, M.A., Talling, P.J., Challenor, P., Malgesini, G. & Hunt, J., 2014. Distal turbidites reveal a common distribution for large (>0.1 $km^3$) submarine landslide recurrence. *Geology* 42, 263–266.

Deng, X., Fu, J., Yao, J., Pang, J. & Sun, B., 2011. Sedimentary facies of the Middle-Upper Triassic Yanchang Formation in Ordos Basin and breakthrough in petroleum exploration. *Journal of Palaeogeograph*y 13, 443–455 (in Chinese with English abstract).

Dong, Y., Liu, X., Zhang, G., Chen, Q., Zhang, X., Li, W. & Yang, C., 2012. Triassic diorites and granitoids in the Foping area: Constraints on the conversion from subduction to collision in the Qinling orogen, China. *Journal of Asian Earth Sciences* 47, 123–142.

Ezquerro, L., Moretti, M., Liesa, C.L., Luzón, A. & Simón, J.J., 2015. Seismites from a well core of palustrine deposits as a tool for reconstructing the palaeoseismic history of a fault. *Tectonophysics* 655, 191–205.

Ezquerro, L., Moretti, M., Liesa, C.L., Luzón, A., Pueyo, E.L. & Simón, J.L., 2016. Controls on space-time distribution of soft-sediment deformation structures: applying palaeomagnetic dating to approach the apparent recurrence period of paleoseisms at the Concud Fault (eastern Spain). *Sedimentary Geology*: 344, 91–111.

Ghosh, S.K., Sengupta, S. & Dasgupta, S., 2002. Tectonic deformation of soft-sediment convolute folds. *Journal of Structural Geology* 24, 913–923.

Gladkov, A.S., Lobova, E.U., Deev, E.V., Korzhenkov, A.M., Mazeika, J.V., Abdieva, S.V., Rogozhin, E.A., Rodkin, M.V., Fortuna, A.B., Charimov, T.A. & Yudakhin, A.S. Earthquake-induced soft-sediment deformation structures in Late Pleistocene lacustrine deposits of Issyk-Kul lake (Kyrgyzstan). *Sedimentary Geology:* 344, 112–122.

Hansen, L., l'Heureux, J.S. & Longva, O., 2011. Turbiditic clay-rich event beds in fjord-marine deposits caused by landslides in emerging clay deposits – palaeoenvironmental interpretation and role for submarine mass-wasting. *Sedimentology* 58, 890–915.

Haughton, P., Davis, C., McCaffrey, W. & Barker, S., 2009. Hybrid sediment gravity flow deposits – classification, origin and significance. *Marine and Petroleum Geology* 26, 1900–1918.

Hovikoski, J., Lemiski, R., Gingras, M., Pemberton, G. & Maceachern, J.A., 2008. Ichnology and sedimentology of a mud-dominated deltaic coast: Upper Cretaceous Alderson Member (Lea Park Fm.), Western Canada. *Journal of Sedimentary Research* 78, 803–824.

Ichaso, A.A. & Dalrymple, R.W., 2009. Tide- and wave-generated fluid mud deposits in the Tilje Formation (Jurassic), offshore Norway. *Geology* 37, 539–542.

Ji, L., Yan, K., Meng, F. & Song, Z., 2010. The oleaginous *Botryococcus* from the Triassic Yanchang Formation in Ordos Basin, Northwestern China: Morphology and its paleoenvironmental significance. *Journal of Asian Earth Sciences* 38, 175–185.

Kelly, R.I. & Martini, I.P., 1986. Pleistocene glacio-lacustrine deltaic deposits of the Scarborough Formation, Ontario, Canada. *Sedimentary Geology* 47, 27–52.

Kirby, R. & Parker, W.R., 1983. Distribution and behavior of fine sediment in the Severn Estuary and inner Bristol Channel, U.K. *Canadian Journal of Fishery and Aquatic Sciences* 40, 83–95.

Kostic, S., 2014. Upper flow regime bedforms on levees and continental slopes: Turbidity current flow dynamics in response to fine-grained sediment waves. *Geosphere* 10, 1094–1103.

Kuenen, Ph.H., 1958. Experiments in geology. *Transactions, Geological Society Glasgow* 23, 1–28

Lamb, M.P. & Mohrig, D., 2009. Do hyperpycnal-flow deposits record river-flood dynamics? *Geology* 37, 1067–1070.

Lowe, D.R. & Guy, M., 2000. Slurry-flow deposits in the Britannia Formation (Lower Cretaceous), North Sea: a new perspective on the turbidity current and debris flow problem. *Sedimentology* 47, 31–70.

Lowe, D.R., Guy, M. & Palfrey, A., 2003. Facies of slurry-flow deposits, Britannia Formation (Lower Cretaceous), North Sea: implications for flow evolution and deposit geometry. *Sedimentology* 50, 45–80.

MacEachern, J.A., Bann, K.L., Bhattacharya, J.P. & Howell, C.D., 2005. Ichnology of deltas: organism responses to the dynamic interplay of rivers, waves, storms and tides. [In:] L. Giosan & J.P. Bhattacharhya (Eds): *River deltas – concepts, models, and examples*. SEPM Special Publications 83, 45–85.

Martín-Chivelet, J., Palma, R.M., López-Gómez, J. & Kietzmann, D.A., 2011. Earthquake-induced soft-sediment deformation structures in Upper Jurassic open-marine microbialites (Neuquén Basin, Argentina). *Sedimentary Geology* 235, 210–221.

Mills P.C., 1983. Genesis and diagnostic value of soft-sediment deformation structures – A review. *Sedimentary Geology* 35, 83–104.

Mulder, T. & Alexander, J., 2001. The physical character of subaqueous sedimentary density flows and their deposits. *Sedimentology* 48, 269–299.

Neill, C.F. & Allison, M.A., 2005. Subaqueous deltaic formation on the Atchafalaya shelf, Louisiana. *Marine Geology* 214, 411–430.

Plint, A.G., 2014. Mud dispersal across a Cretaceous prodelta: Storm-generated, wave-enhanced sediment gravity flows inferred from mudstone microtexture and microfacies. *Sedimentology* 61, 609–647.

Pouderoux, H., Proust, J., Lamarche, G., Orpin, A. & Neil, H., 2012. Postglacial (after 18 ka) deep-sea sedimentation along the Hikurangi subduction margin (New Zealand): Characterisation, timing and origin of turbidites. *Marine Geology* 295/298, 51–76.

Rodríguez-López, J.P., Meléndez, N., Soria, A.R., Liesa, C.L. & Van Loon, A.J., 2007. Lateral variability of ancient seismites related to differences in sedimentary facies (the synrift Escucha Formation, mid-Cretaceous, eastern Spain). *Sedimentary Geology* 201, 461–484.

Schieber, J., 1994. Evidence for episodic high energy events and shallow water deposition in the Chatta-

nooga Shale, Devonian, central Tennessee, U.S.A. *Sedimentary Geology* 93, 193–208.

Schieber, J., Southard, J.B. & Thaisen, K., 2007. Accretion of mudstone beds from migrating floccule ripples. *Science* 318, 1760–1763.

Sumner, E.J., Talling, P.J. & Amy, L.A., 2009. Deposits of flows transitional between turbidity current and debris flow. *Geology* 37, 991–994.

Sumner, E.J., Talling, P.J. & Amy, L.A., 2012. Facies architecture of individual basin-plain turbidites: Comparison with existing models and implications for flow processes. *Sedimentology* 59, 1850–1887.

Sumner, E.J., Siti, M.I., McNeill, L.C., Talling, P.J., Henstock, T.J., Wynn, R.B., Djajadihardja, Y.S. & Permana, H., 2013. Can turbidites be used to reconstruct a paleoearthquake record for the central Sumatran margin? *Geology* 41, 763–766.

Sylvester, Z. & Lowe, D.R., 2004. Textural trends in turbidites and slurry beds from the Oligocene flysch of the East Carpathians, Romania. *Sedimentology* 51, 945–972.

Talling, P.J., Wynn, R.B., Masson, D.G., Frenz, M., Cronin, B.T., Schiebel, R., Akhmetzhanov, A.M., Dallmeier-Tiessen, S., Benetti, S., Weaver, P.P.E., Georgiopoulou, A., Zühlsdorff, C. & Amy, L.A., 2007. Onset of submarine debris flow deposition far from original giant landslide. *Nature* 450, 541–544.

Törő, B. & Pratt, B.R., 2016. Sedimentary record of seismic events in the Eocene Green River Formation and its implications for regional tectonics on lake evolution (Bridger Basin). *Sedimentary Geology*: 344, 175–204.

Van Loon, A.J., 2002. Soft-sediment deformations in the Kleszczów Graben (central Poland). *Sedimentary Geology* 147, 57–70.

Van Loon, A.J. & Wiggers, A.J., 1975. Holocene lagoonal silts (formerly called "sloef") from the Zuiderzee. *Sedimentary Geology* 13, 47–55.

Van Loon, A.J. & Wiggers, A.J., 1976. Metasedimentary "graben" and associated structures in the lagoonal Almere Member (Groningen Formation, The Netherlands). *Sedimentary Geology* 16, 237–254.

Weislogel, A.L., Graham, S.A., Chang, E.Z., Wooden, J.L., Gehrels, G.E. & Yang, H., 2006. Detrital zircon provenance of the Late Triassic Songpan-Ganzi complex: Sedimentary record of collision of the North and South China blocks. *Geology* 34, 97–100.

Yamamoto, Y., 2014. Dewatering structure and soft-sediment deformation controlled by slope instability: examples from the late Miocene to Pliocene Miura–Boso accretionary prism and trench-slope basin, central Japan. *Marine Geology* 356, 65–70.

Yang, H. & Deng, X., 2013. Deposition of Yanchang Formation deep-water sandstone under the control of tectonic events, Ordos Basin. *Petroleum Exploration and Development* 40, 513–520.

Yang, R.C., He, Z.L., Qiu, G.Q., Jin, Z.J., Sun, D.S. & Jin, X.H., 2014. A Late Triassic gravity flow depositional system in the southern Ordos Basin. *Petroleum Exploration and Development* 41, 724–733.

Yang, R., Jin, Z., Van Loon, A.J., Han, Z. & Fan, A., 2016. Climatic and tectonic controls of lacustrine hyperpycnite origination in the Late Triassic Ordos Basin, central China: implications for unconventional petroleum development. *American Association of Petroleum Geologists Bulletin* (in press; preliminary version published online Ahead of Print 25 July 2016; DOI:10.1306/06101615095).

Yao, Y., Flemings, P. & Mohrig, D., 2012. Dynamics of dilative slope failure. *Geology* 40, 663–666.

Zou, C., Wang, L., Li, Y., Tao, S. & Hou, L., 2012. Deep-lacustrine transformation of sandy debrites into turbidites, Upper Triassic, Central China. *Sedimentary Geology* 265/266, 143–155.

*Manuscript received: 20 September 2016*
*Revision accepted: 3 November 2016*